Direct observation of double exchange in ferromagnetic $La_{0.7}Sr_{0.3}CoO_3$ by broadband ellipsometry

P. Friš, D. Munzar, O. Caha, and A. Dubroka*

Department of Condensed Matter Physics, Faculty of Science and Central European Institute of Technology, Masaryk University, Kotlářská 2, 611 37 Brno, Czech Republic

(Received 11 July 2017; revised manuscript received 11 December 2017; published 19 January 2018)

We present results of our broadband ellipsometry measurements of the optical response of ferromagnetic $La_{0.7}Sr_{0.3}CoO_3$. Our data show that the ferromagnetic transition is accompanied by a transfer of optical spectral weight from an absorption band centered at 1.5 eV to a narrow component of the Drude-like peak. The associated reduction of the intraband kinetic energy is significantly larger than $k_B T_c$, confirming that the double exchange plays a major role in the ferromagnetism of doped cobaltites. In conjunction with results of recent theoretical studies, the temperature dependence of the Drude-like peak suggests that the double exchange is mediated by t_{2g} orbitals.

DOI: 10.1103/PhysRevB.97.045137

Transition metal oxides with the perovskite structure are well known for their spectacular electronic and magnetic properties such as superconductivity in cuprates and colossal magnetoresistance associated with the ferromagnetic transition in hole doped manganites [1]. While consensus has been reached that the ferromagnetism in the manganites is caused by the double exchange (DE) mechanism mediated by e_g electrons, the origin of ferromagnetism in related pseudocubic cobaltites $La_{1-x}Sr_xCoO_3$ ($0.2 < x < 0.5$), with comparable values of the Curie temperature (T_c) reaching up to 250 K, is still being debated [2–8]. The physics of the cobaltites is considerably complicated by a quasidegeneracy between several spin states of a Co ion. This is caused by a competition between the Hund's rule coupling and the crystal field splitting [9]. In this context, it is of high importance to find out whether the cobaltites exhibit optical signatures of the DE comparable to those observed in the manganites. Recall that the hallmark of the DE mechanism in the manganites is a lowering of the effective kinetic energy of charge carriers occurring upon the transition from the paramagnetic (PM) to the ferromagnetic (FM) state [10]. It manifests itself in the optical conductivity as a transfer of spectral weight (SW) from a band at a finite energy in the PM state to the Drude-like peak in the FM state [11]. The band is due to the so-called wrong spin transition (WST) [12–14] arising from hopping of carriers between sites with misaligned spins [11–17].

In order to explore possible optical signatures of DE and contribute to the clarification of the mechanism of ferromagnetism in hole doped cobaltites, we have measured their optical response as a function of temperature (T) using broadband ellipsometry. The early optical study of doped cobaltites by Tokura *et al.* [18] is limited to room temperature. We observed the SW transfer between a WST band and the Drude-like peak similar to the one reported in manganites. The fact that the associated reduction of the intraband kinetic energy is significantly larger than $k_B T_c$, demonstrates that ferromagnetism in cobaltites is indeed driven by a DE mechanism.

30 nm thin film of $La_{0.7}Sr_{0.3}CoO_3$ (LSCO) was grown by pulsed laser deposition (PLD) on 10×10 mm^2 substrates $(La_{0.7}Sr_{0.3}) \times (Al_{0.65}Ta_{0.35})O_3$ (LSAT) [19]. The samples were annealed *in situ* at the deposition temperature of 650 °C under 10 Torr oxygen pressure to decrease oxygen vacancy concentration [19]. X-ray diffraction measurements confirmed that the film is epitaxial, see the Supplemental Material (SM) [20]. Broadband ellipsometry measurements were performed using three ellipsometers: Woollam VASE ellipsometer (0.6–6.5 eV), Woollam IR-VASE ellipsometer (0.08–0.65 eV), and an in-house built ellipsometer for the far-infrared range (0.01–0.08 eV) [21]. For each measured photon energy value, the optical conductivity of the film was obtained from the ellipsometric angles Ψ and Δ using the model of coherent interferences in a layer on a substrate. The optical response of the substrate was measured on a bare substrate. In this way, the optical response was obtained without extrapolations needed for a Kramers-Kronig analysis used, e.g., in reflectivity data analysis. The film thickness was determined using ellipsometry and x-ray diffraction. The magnetic moments were measured using a vibrating sample magnetometer.

The resulting spectra of the real part of the optical conductivity σ_1 of LSCO deposited on LSAT are shown in Fig. 1(a) for $T = 200$ K close to $T_c = 205$ K and for the lowest T of our measurements (7 K). Figures 1(b) and 1(c) show all measured spectra on a magnified scale. The values of $\sigma_1(\omega)$ for energies lower than 0.01 eV were obtained using extrapolations based on a Kramers-Kronig consistent model introduced below. The corresponding spectra of the PLD target were found to be very similar [20]. The spectra of σ_1 exhibit a Drude-like peak at low energies and two absorption bands centered around 2.3 and 5.1 eV, see Fig. 1(a). Based on the results of Ref. [22], we assign the absorption band centered at 2.3 eV to the O $2p$ to Co $3d$ charge transfer transition. At low T, σ_1 exhibits metallic behavior with fairly high values of $\sigma_1(0)$ reaching $\sim 8000\ \Omega^{-1}\,\mathrm{cm}^{-1}$ for $T \to 0$ [see Fig. 1(b)], but even above $T_c \sim 200$ K, the

*dubroka@physics.muni.cz

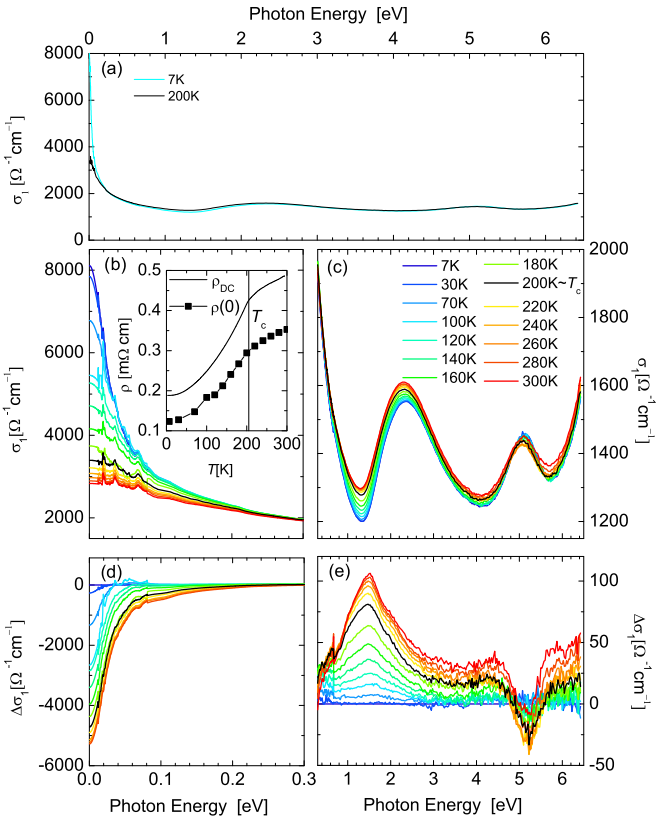

FIG. 1. The real part of the optical conductivity $\sigma_1(\omega)$ of $La_{0.7}Sr_{0.3}CoO_3$ deposited on LSAT. (a) $\sigma_1(\omega)$ at $T = 200$ K $\approx T_c$ and at 7 K. (b) and (c) $\sigma_1(\omega)$ for all measured temperatures on a magnified scale. The inset of (b) shows the T dependencies of $\rho(0) = 1/\sigma_1(0)$ and of the dc resistivity ρ_{dc}. (d) and (e) $\Delta\sigma_1(\omega,T) \equiv \sigma_1(\omega,T) - \sigma_1(\omega,7\text{ K})$.

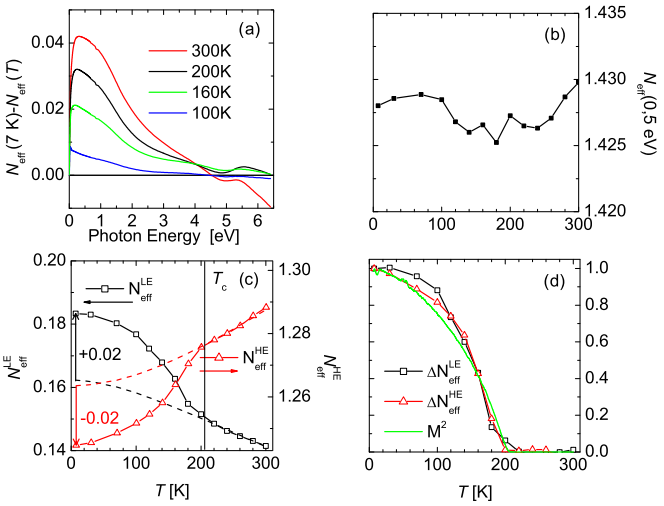

FIG. 2. (a) Energy dependence of the quantity $N_{\text{eff}}(0,\omega,7\text{ K}) - N_{\text{eff}}(0,\omega,T)$ introduced in the text. (b) Temperature dependence of the spectral weight $N_{\text{eff}}(0,5\text{ eV},T)$. (c) T dependencies of the low and high energy spectral weights $N_{\text{eff}}^{\text{LE}} = N_{\text{eff}}(0,0.3\text{ eV})$ and $N_{\text{eff}}^{\text{HE}} = N_{\text{eff}}(0.3,5\text{ eV})$. Estimates for the background T dependencies discussed in the text are shown as the dashed lines. (d) Absolute values of the differences $\Delta N_{\text{eff}}^{\text{LE}}$ and $\Delta N_{\text{eff}}^{\text{HE}}$ between the spectral weights and the corresponding background T dependencies together with the square of the magnetization measured at $B = 20$ mT. All quantities are normalized to their lowest temperature values.

low frequency response is still very metallic with high values of $\sigma_1(0)$ of $\sim 3000\ \Omega^{-1}\,\text{cm}^{-1}$. The spectra do not exhibit any signatures of Jahn-Teller localization (for details, see the SM [20]), in agreement with results of Ref. [23]. The inset of Fig. 1(b) displays the T dependencies of $\rho(0) = 1/\sigma_1(0)$ and the directly measured dc resistivity ρ_{dc}. The values of $\rho(0)$ agree within 30% with the resistivity measured on a single crystal [24], which demonstrates that our thin film is of high quality and indicates that its optical properties are fairly close to the bulk ones. The magnitude of ρ_{dc} is by a factor of about 1.4 larger than that of $\rho(0)$ which is an effect typically observed on thin films due to linear defects [12]. The T dependencies of ρ_{dc} and $\rho(0)$ display a clear anomaly at $T_c \sim 205$ K similar to that of the single crystal [24], indicating that double exchange should be considered as a plausible mechanism for the magnetic ordering.

Next, we address in detail the T dependence of σ_1. Figures 1(d) and 1(e) show differential spectra $\Delta\sigma_1(\omega,T) \equiv \sigma_1(\omega,T) - \sigma_1(\omega,7\text{ K})$. With increasing temperature, $\Delta\sigma_1$ strongly decreases below 0.1 eV and, on the contrary, a band is formed with the maximum at $\sim$1.5 eV. This is analogous to the DE related SW redistribution occurring in manganites, where the FM $\rightarrow$ PM transition is associated with a SW transfer from the Drude peak to a band centered at 3.2 eV [12,13].

We quantified the frequency and T dependence of the optical SW in terms of the effective number of charge carriers per unit cell N_{eff}, defined as

$$N_{\text{eff}}(\omega_L,\omega_H) = \frac{2m_0V}{\pi e^2}\int_{\omega_L}^{\omega_H}\sigma_1(\omega)d\omega, \qquad (1)$$

where m_0 is the electron mass, V is unit cell volume, and e is the electron charge. The quantity $N_{\text{eff}}(\omega_L,\omega_H)$ represents an estimate for the number of charge carriers per unit cell responsible for absorption between ω_L and ω_H. Figure 2(a) displays the energy dependence of the difference $N_{\text{eff}}(0,\omega,T = 7\text{ K}) - N_{\text{eff}}(0,\omega,T)$ demonstrating that the SW between 0 and $\hbar\omega_H = 5$ eV is essentially temperature independent. Figure 2(b) confirms that the T dependence of $N_{\text{eff}}(0,5\text{ eV})$ is very weak. Figures 1(b) and 1(c) show that the data exhibit an isosbestic point (a point where σ_1 is almost T independent) at $\hbar\omega = 0.3$ eV. Motivated by this finding, we plot in Fig. 2(c) the T dependence of the low energy SW $N_{\text{eff}}^{\text{LE}}$, defined as $N_{\text{eff}}(0,\ 0.3\text{ eV})$, and that of the high energy SW $N_{\text{eff}}^{\text{HE}}$, defined as $N_{\text{eff}}(0.3\text{ eV},5\text{ eV})$. Both quantities display a pronounced anomaly at $T \approx 200$ K $\approx T_c$. This finding demonstrates that a part of the SW transfer between high and low energies is due to the FM transition and implies that the onset of the FM order is associated with a kinetic energy saving characteristic of the DE mechanism.

The T dependencies of the SWs in Fig. 2(c) are, in addition to the DE, influenced by a common narrowing of the Drude peak due to the increase of the quasiparticle lifetime with decreasing T. We attempted to separate the two contributions by approximating the "normal" components of the T dependencies with extrapolations based on fits of the high

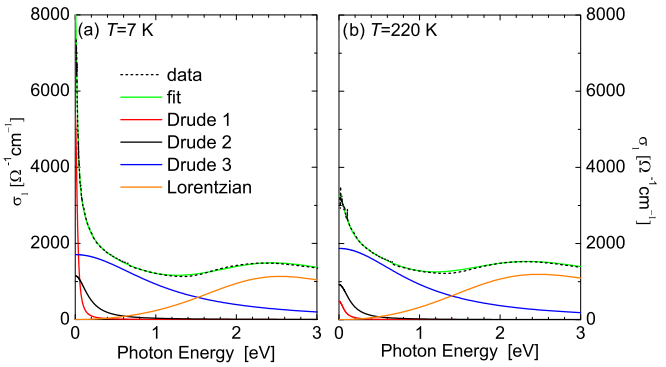

FIG. 3. Measured $\sigma_1(\omega)$ (dotted line), model spectrum (solid green line), and contributions of individual terms in Eq. (2) for $T = 7$ K (a) and for $T = 220$ K (b).

temperature segments using a background function [20]. In Fig. 2(c) they are represented by the dashed lines. The estimated magnitude of the DE related contribution $N_{\rm eff}^{\rm DE}$ [see the vertical arrows in Fig. 2(c)], is approximately 0.02. Figure 2(d) displays the T dependencies of $\Delta N_{\rm eff}^{\rm LE}$, $\Delta N_{\rm eff}^{\rm HE}$ (the SWs with the background contributions subtracted) together with the T dependence of M^2, where M is the measured magnetization. The T dependencies are very similar which indicates that the observed FM related SW changes are connected to the energetics of the FM transition [10].

In order to obtain additional insight into the optical response, we modeled the complex conductivity $\sigma(\omega) = -i\epsilon_0\omega[\epsilon(\omega) - 1]$ using the Drude-Lorentz model of the dielectric function

$$\epsilon(\omega) = 1 - \sum_j \frac{\omega_{D,j}^2}{\omega(\omega + i\gamma_{D,j})} + \sum_k \frac{\omega_{L,k}^2}{\omega_{0,k}^2 - \omega^2 - i\omega\gamma_{L,k}}, \tag{2}$$

where the second and the third terms on the right side represent the Drude and the Lorentz contributions, respectively, parameters $\omega_{D,j}$ and $\omega_{L,k}$ are plasma frequencies, $\gamma_{D,j}$ and $\gamma_{L,k}$ are broadening parameters, and $\omega_{0,k}$ are frequencies of the Lorentz terms. Figures 3(a) and 3(b) show the experimental data and fits for $T = 7$ and 220 K $> T_c$ on a magnified scale. The complete set of obtained parameter values can be found in the SM [20]. It turns out that the interband transitions at 2.3 and 5.1 eV can be represented by only one Lorentz term per transition. However, in order to obtain a reasonable fit of the free carrier response, three Drude terms are required with $\hbar\gamma_D = 0.03$, 0.17, and 1 eV at 7 K (0.07, 0.15, and 1 eV at 220 K) and with the corresponding SWs proportional to $(\hbar\omega_D)^2 = 1.1$, 1.5, and 14 eV^2 at 7 K (0.25, 1.0, and 14 eV^2 at 220 K), respectively. It appears that only the two narrower Drude terms change significantly with T, whereas the broadest Drude term is almost T independent.

This behavior can be qualitatively understood based on results of a recent LDA+DMFT study [25], which indicates that both e_g and t_{2g} bands cross the chemical potential. The e_g band has a large bandwidth and its quasiparticles are strongly damped by correlations and the corresponding broadening of the spectral function is about 0.6 eV. In contrast, the t_{2g} band has a relatively small bandwidth and its quasiparticles are much less damped, with the broadening of about 0.04 eV. In view of these results we suggest that the broadest Drude term mainly corresponds to the response of the e_g bands and the two narrower Drude terms correspond to the response of the t_{2g} bands. The SW of the broadest Drude term is about 5 times higher than the sum of the SWs of the two narrower Drude terms, which correlates with the large difference between the predicted (e.g., in Ref. [25]) bandwidths of the two channels.

Note that in manganites at low temperature, the Drude peak is also composed of a narrow and a broad component [14]. However, the components exhibit a similar and pronounced temperature dependence, which suggests that they originate from the same band. Relatively, the sum of the SWs of the two narrower Drude terms increases by a factor of 2 when going from T_c to the lowest temperature, which is comparable to the twofold increase of the intraband SW occurring in manganites [12]. The magnitude of the total SW transfer upon the FM transition, $N_{\rm eff}^{\rm DE} = 0.02$, is approximately 7 times lower than the one observed in manganites [12–14], for details see the SM [20]. This difference is presumably due to the narrow bandwidth of the t_{2g} bands compared to the e_g bands in manganites. The fact that below T_c spectral weight $N_{\rm eff}^{\rm DE}$ is transferred only to the narrow component of the Drude peak is consistent with the DE mediated by t_{2g} electrons, as recently suggested [2,4]. The associated saving of the intraband kinetic energy $\Delta K = 3\hbar^2 N_{\rm eff}^{\rm DE}/a_0^2 m_0$ [20,26], where $a_0 = 3.82$ Å is the pseudocubic lattice parameter, is about 30 meV. Albeit smaller than in manganites, this value is larger than $k_B T_c \approx 17$ meV, which shows that the kinetic energy reduction plays an important role in the mechanism of ferromagnetism in doped cobaltites.

Next, we address the origin and the properties of the 1.5 eV band in Fig. 1(e). As discussed above, the T dependence of its SW correlates with that of the narrow Drude peak, in a way remarkably similar to that of the WST feature in manganites. Based on this observation we suggest that the 1.5 eV band is also a result of a WST. To clarify the nature of this WST, we first consider, for the sake of simplicity, weakly coupled pairs of Co sites with well defined spin states [27]. Examples of corresponding WST from a Co^{3+} ion to a Co^{4+} ion are shown in Fig. 4. The abbreviations IS and HS in the Co^{3+} column [LS, IS, and HS in the Co^{4+} column] stand for the intermediate ($t_{2g}^5\ e_g^1$) and high spin ($t_{2g}^4\ e_g^2$) configurations of Co^{3+} [low ($t_{2g}^5\ e_g^0$), intermediate ($t_{2g}^4\ e_g^1$), and high spin ($t_{2g}^3\ e_g^2$) configurations of Co^{4+}]. The WSTs, indicated by the long arrows, result in excited states with one unpaired electron whose spin is oriented antiparallel to those of other unpaired electrons at the same site. Note that the optical process preserves the electron spin. For comparison, the bottom panel of Fig. 4 shows the WST between Mn^{3+} and Mn^{4+} occurring in manganites. Finally, the energies $E^{\rm WST}$ of the WST and the average values of the magnetic moment μ per transition metal site are given in the second and the third columns, respectively. The energies have been obtained using the Hund's rule coupling Hamiltonian [28]

$$H = -J_{\rm H} \sum_{l,l',l\neq l'} \mathbf{S}_l \mathbf{S}_{l'}, \tag{3}$$

where the sum runs over all pairs l,l' of $3d$ orbitals, $J_{\rm H}$ is the coupling constant, and $\mathbf{S}_l$ is the spin operator for the orbital l. Clearly the WST appears due to the presence of

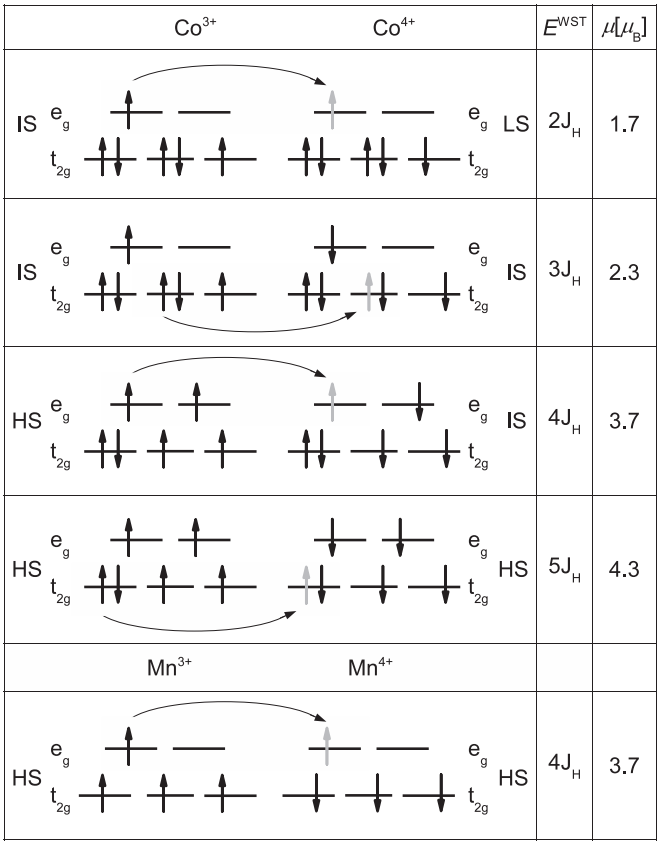

FIG. 4. Examples of wrong spin transitions, in the ionic limit, between a Co^{3+} site and Co^{4+} site for various Co spin states. Transition energy values E^{WST} and the average magnetic moments μ per site computed for 30% hole doping. The lowest row shows the corresponding situation in $La_{0.7}Sr_{0.3}MnO_3$.

pairs of transition metal sites with misaligned spins. In the FM phase, the complete alignment of spins allows for the coherent transport of charge carriers. The WST is absent and the spectral weight it had in the PM state is transferred to the Drude peak. The corresponding lowering of the effective kinetic energy is the essence of the DE mechanism. Note that the value of E^{WST} can be reduced with respect to that expected within the ionic limit due to a partially itinerant character of charge carriers. For manganites, this has been suggested to reduce the value of E^{WST} from $4J_H$ to approximately $2J_H$ [15–17,29].

Importantly, in Fig. 4 E^{WST} is approximately proportional to μ. Provided the values of J_H(Co) and J_H(Mn) are approximately the same, the values of E^{WST}/μ for LSCO and LCMO can be expected to be similar. Indeed, for LSCO the experimental values $E^{WST}_{LSCO} = 1.5$ eV and $\mu \approx 1.5\ \mu_B$ [3,20] yield $E^{WST}/\mu = 1.0\,\text{eV}/\mu_B$, which is comparable to the value of $0.8\,\text{eV}/\mu_B$ for LSMO. The latter has been obtained using $E^{WST}_{LSMO} = 3.2$ eV [12] and $\mu_{LSMO} \approx 3.6\ \mu_B$ [30]. In the most simple picture, the facts that E^{WST}_{LSCO} is about one half of E^{WST}_{LSMO} and that $\mu_{LSCO} \approx 1.5\ \mu_B$ would point to the first row of Fig. 4. Results of a recent x-ray study [2], however, indicate that the Co ions are partially in the LS and partially in the HS configuration, rather than in the IS one. This point of view is supported by the LDA+DMFT study [25], which argues that the average occupations of HS-related and LS-related states are approximately 30% and 70%, respectively [25]. This offers the following qualitative picture of the DE in cobaltites: the DE is connected to the HS states and meditated by the t_{2g} electrons. As a consequence of the admixture of low spin states, E^{WST} can be expected to be considerably lower than $5J_H$ of the extreme HS-HS case (shown in the fourth row in Fig. 4).

In summary, we have observed that the ferromagnetic transition in $La_{0.7}Sr_{0.3}CoO_3$ is associated with a transfer of spectral weight from an absorption band centered at 1.5 eV to a narrow component of the Drude peak. Similarly to the manganites, the band can be interpreted in terms of a wrong spin transition involving Co sites with misaligned spins. Its energy is lower than that of the corresponding band in manganites which is consistent with a lower value of the ordered magnetic moment. The fact that the FM influences only the narrow and relatively weak component of the Drude peak, in conjunction with results of a recent theoretical study [25], suggests that the double exchange is mediated by t_{2g} orbitals. The associated reduction of the intraband kinetic energy is significantly larger than $k_B T_c$, confirming that the double exchange is indeed at the heart of ferromagnetism in doped cobaltites.

We acknowledge helpful discussions with J. Chaloupka, D. Fuchs, G. Khaliullin, and K. Knížek and magnetic measurements at IPM ASCR supervised by M. Hapla. This work was financially supported by the MEYS of the Czech Republic under the project CEITEC 2020 (LQ1601) and carried out with the support of CEITEC Nano Research Infrastructure (MEYS CR, 2016–2019). P.F. and D.M. were supported by projects MUNI/A/1310/2016 and MUNI/A/1291/2017.

[1] Y. Tokura, Rep. Prog. Phys. **69**, 797 (2006).
[2] M. Merz, P. Nagel, C. Pinta, A. Samartsev, H. v Löhneysen, M. Wissinger, S. Uebe, A. Assmann, D. Fuchs, and S. Schuppler, Phys. Rev. B **82**, 174416 (2010).
[3] D. Samal and P. S. A. Kumar, J. Phys.: Condens. Matter **23**, 016001 (2011).
[4] D. Fuchs, M. Merz, P. Nagel, R. Schneider, S. Schuppler, and H. von Löhneysen, Phys. Rev. Lett. **111**, 257203 (2013).
[5] Z. Othmen, A. Schulman, K. Daoudi, M. Boudard, C. Acha, H. Roussel, M. Oueslati, and T. Tsuchiya, Appl. Surf. Sci. **306**, 60 (2014).
[6] A. V. Lazuta, V. A. Ryzhov, V. V. Runov, V. P. Khavronin, and V. V. Deriglazov, Phys. Rev. B **92**, 014404 (2015).
[7] R. X. Smith, M. J. R. Hoch, W. G. Moulton, P. L. Kuhns, A. P. Reyes, G. S. Boebinger, H. Zheng, and J. F. Mitchell, Phys. Rev. B **93**, 024204 (2016).

[8] B. Li, R. V. Chopdekar, A. T. N'Diaye, A. Mehta, J. P. Byers, N. D. Browning, E. Arenholz, and Y. Takamura, Appl. Phys. Lett. **109**, 152401 (2016).
[9] S. Maekawa, T. Tohyama, S. E. Barnes, S. Ishihara, W. Koshibae, and G. Khaliullin, *Physics of Transition Metal Oxides* (Springer, Berlin, 2004).
[10] S. Blundell, *Magnetism in Condensed Matter* (Oxford University Press, New York, 2001).
[11] Y. Okimoto, T. Katsufuji, T. Ishikawa, A. Urushibara, T. Arima, and Y. Tokura, Phys. Rev. Lett. **75**, 109 (1995).
[12] M. Quijada, J. Cerne, J. R. Simpson, H. D. Drew, K. H. Ahn, A. J. Millis, R. Shreekala, R. Ramesh, M. Rajeswari, and T. Venkatesan, Phys. Rev. B **58**, 16093 (1998).
[13] K. Takenaka, Y. Sawaki, R. Shiozaki, and S. Sugai, Phys. Rev. B **62**, 13864 (2000).
[14] K. Takenaka, R. Shiozaki, and S. Sugai, Phys. Rev. B **65**, 184436 (2002).
[15] N. Furukawa, J. Phys. Soc. Jpn. **64**, 3164 (1995).
[16] A. Chattopadhyay, A. J. Millis, and S. Das Sarma, Phys. Rev. B **61**, 10738 (2000).
[17] B. Michaelis and A. J. Millis, Phys. Rev. B **68**, 115111 (2003).
[18] Y. Tokura, Y. Okimoto, S. Yamaguchi, H. Taniguchi, T. Kimura, and H. Takagi, Phys. Rev. B **58**, R1699 (1998).
[19] By Alineason Materials Technology GmbH, Germany.
[20] See Supplemental Material at http://link.aps.org/supplemental/10.1103/PhysRevB.97.045137 for details on X-ray diffraction data, Jahn-Teller localisation, saturated magnetic moment, spectral weight considerations and optical data from polycrystalline LSCO. The supplemental material includes Refs. [31,32].
[21] P. Friš and A. Dubroka, Appl. Surf. Sci. **421**, 430 (2017).
[22] D. W. Jeong, W. S. Choi, S. Okamoto, J.-Y. Kim, K. W. Kim, S. J. Moon, D.-Y. Cho, H. N. Lee, and T. W. Noh, Sci. Rep. **4**, 06124 (2014).
[23] N. Sundaram, Y. Jiang, I. E. Anderson, D. P. Belanger, C. H. Booth, F. Bridges, J. F. Mitchell, T. Proffen, and H. Zheng, Phys. Rev. Lett. **102**, 026401 (2009).
[24] H. M. Aarbogh, J. Wu, L. Wang, H. Zheng, J. F. Mitchell, and C. Leighton, Phys. Rev. B **74**, 134408 (2006).
[25] P. Augustinský, V. Křápek, and J. Kuneš, Phys. Rev. Lett. **110**, 267204 (2013).
[26] D. N. Basov and T. Timusk, Rev. Mod. Phys. **77**, 721 (2005).
[27] For a related analysis of intersite excitations in t_{2g}^n systems ($n = 1$–5), see J. Lee, M. Kim, and T. Noh, New J. Phys. **7**, 147 (2005).
[28] By Hund's rule coupling Hamiltonian we mean the spin-spin coupling term of the five band Hubbard Hamiltonian given, e.g., in A. M. Oleś, Phys. Rev. B **28**, 327 (1983).
[29] C. Lin and A. J. Millis, Phys. Rev. B **78**, 174419 (2008).
[30] M. C. Martin, G. Shirane, Y. Endoh, K. Hirota, Y. Moritomo, and Y. Tokura, Phys. Rev. B **53**, 14285 (1996).
[31] Y. Okimoto, T. Katsufuji, T. Ishikawa, T. Arima, and Y. Tokura, Phys. Rev. B **55**, 4206 (1997).
[32] J. P. Prieto-Ruiz, F. M. Romero, H. Prima-Garcia, and E. Coronado, J. Mater. Chem. C **3**, 11122 (2015).